NURETH14-369

PREDICTION OF BOILING-INDUCED NATURAL CIRCULATION FLOW IN AN INCLINED CHANNEL WITH NON-UNIFORM FLOW AREA

Kwang Soon Ha^{1*}, Fan-Bill Cheung², Jinho Song¹, Rae Joon Park¹ and Sang Baik Kim¹

¹ Korea Atomic Energy Research Institute, Daejeon, Korea ² Pennsylvania State University, University Park, Pennsylvania, USA

Abstract

The boiling-induced natural circulation flow in the engineered cooling channel is modelled and solved by considering the conservation of mass, momentum and energy in the two-phase mixture, along with the two-phase friction drop and void fraction. The model has been applied to estimate the induced mass flow rates through a uniform and non-uniform annular gap between the reactor vessel and insulation under the IVR-ERVC conditions, and also the engineered corium cooling system of an ex-vessel core catcher during a severe accident for various system parameters including the channel gap size, inlet diameter, inlet subcooling, and wall heat flux.

Introduction

Various safety systems are designed and adapted in nuclear power plants to prevent postulated accidents, and to enhance the life time and economic benefit, and finally to increase a public acceptance of the plants. Postulated severe core damage accidents have a high threat risk for the safety of human health and jeopardize the environment. Versatile measures have been suggested and applied to mitigate severe accidents in nuclear power plants. In-vessel corium retention (IVR) through the external reactor vessel cooling (ERVC) is known to be an effective means for maintaining the integrity of a reactor vessel during a severe accident in a nuclear power plant. Under IVR-ERVC conditions, it is necessary to assure that the heat transfer from the reactor vessel wall to the coolant in the reactor cavity is sufficient to cool and retain the molten corium inside the reactor vessel, especially for high-power reactors. If the molten core debris could not be retained inside the reactor vessel during a postulated severe accident, the molten core debris ejected from the reactor vessel would attack the concrete wall and basement of the reactor cavity. In this case, an ex-vessel corium cooling system associated with the use of an external core catcher should be required for the catching and long-term cooling of the molten corium outside the reactor vessel.

To improve the thermal margin for IVR-ERVC and/or ex-vessel core catchers in high-power reactors, engineered corium cooling systems involving boiling-induced two-phase natural circulation have been proposed to increase the decay heat removal rate. The boiling-induced natural circulation flow is generated in a coolant path between a hot vessel wall and cold coolant

_

^{*} Corresponding author on sabbatical at the Pennsylvania State University

reservoir. In general, an increase in the natural circulation mass flow rate of the coolant leads to an increase in the critical heat flux (CHF) on the hot wall.

According to IVR-ERVC strategy, the coolant is filled up to the designed level outside the reactor vessel before the molten corium is relocated to the lower head vessel. A two-phase natural circulation flow between the reactor vessel wall and its surrounding insulation material is induced by decay heating of the wall. The coolant flows into the gap between the reactor vessel wall and the insulation through water inlets located on the lower bottom insulation plate. The heated two-phase mixture flows out of the gap through outlets on the side or top of the insulation. The induced natural circulation flow is dependent on the configuration of the engineered cooling system including the water inlet area and position, coolant (water and steam) outlet area and position, and the gap geometry between the reactor vessel and the insulation material.

The engineered corium cooling system of an ex-vessel core catcher under consideration is a passive system consisting of an inclined engineered cooling channel made of a single channel between the body of the core catcher and the inside wall of the reactor cavity. Under severe accident conditions, water is supplied from the IRWST to the engineered cooling channel. The water in the inclined channel absorbs the decay heat transferred from the corium through the carbon steel structure of the core catcher body and boils off as steam. The latter is subsequently released into the free volume of the containment above the corium spreading compartment. Water continues to flow from the IRWST to the cooling channel as a result of buoyancy-driven natural circulation. The engineered cooling channel is designed to provide effective long-term cooling and stabilization of the corium mixture in the core catcher body while facilitating steam venting. To maintain the integrity of the ex-vessel core catcher, however, it is required that the water coolant be circulated at a sufficiently high rate through the inclined cooling channel for decay heat removal by downward facing boiling of the water circulated from the IRWST.

In this paper, a one-dimensional steam venting model is employed to predict the behavior of a buoyancy-driven upward co-current two-phase flow in an inclined channel with a non-uniform gap size that simulates the two-phase flow situation in the engineered corium cooling system. The boiling-induced natural circulation flow in the inclined engineered cooling channel is modeled by considering the conservation of mass, momentum and energy in the two-phase mixture, along with the two-phase friction drop and void fraction. The resulting governing system is solved numerically to predict the natural circulation flow rate that would be induced in the channel by the downward-facing boiling process with the flow area and the inclination of the channel relative to the gravitational field as the key parameters. The numerical model is employed to determine the induced mass flow rate through the gap between the reactor vessel and the insulation under IVR-ERVC conditions, and the induced mass flow rate through an inclined gap in the engineered corium cooling system of an ex-vessel core catcher having various design parameters.

1. Analysis of two-phase natural circulation flow

The two-phase flow is analysed to predict the natural circulation mass flow rate occurring in the engineered corium cooling system. Assuming the flow to be at a steady state in the coolant channel, the mass, momentum, and energy equations can readily be formulated. Since no mass is

being added to the flow from outside the channel other than at the inlet, the overall mass flow rate is the sum of the liquid and vapour mass flow rate as given by equation (1). The momentum equation is rearranged by using force balances, that is, the pressure difference along the z-direction can be represented as the sum of the inertia force, gravitational force, wall friction loss induced by the flow, form loss by the geometric change of flow path, and flow loss due to two phase retardation such as the velocity difference between the liquid and vapour phase as given by equation (2). In this study, the flow loss due to two phase retardation is ignored since the two-phase pressure loss is usually much smaller than other loss terms [1]. If the energy losses are ignored through the flow channel, the energy equation can simply be represented by a balance between the flow enthalpy change and the heat input through the heated channel wall as given by equation (3).

The wall friction loss induced by one- or two- phase flow in dynamic equilibrium state can be described by equation (4), assuming only the liquid or the vapour phase to be flowing in the original channel with their respective mass flow rates. The friction factor, f, depends on the Reynolds number of each phase. The values of C and m for evaluating the friction factor given by equation (5) depend on the type of flow taking place inside the channel. The values of C and C are greater than 2300.

The mixture quality is defined as the flow enthalpy change due to the wall heat input as given by equation (6). A method for predicting the void fraction is essential for predicting the acceleration and gravitational components of the pressure gradient in the two phase flow. Butterworth [2] has shown that several of the available void-fraction correlations can be cast in the general form given by equation (7). The values of the various constants in this relation corresponding to different correlations are listed in Table 1 [3].

If the momentum equation is integrated over the entire circulating flow loop from the inlet to the outlet and then back to the inlet, the result must be zero as shown in equation (8). As such, the circulation mass flow rate can be obtained by solving the loop integral equation (8) numerically. Numerical computations have been carried out accordingly. Results are presented in next section.

$$\dot{m} = \rho_m u_m A = \dot{m}_f + \dot{m}_g \tag{1}$$

$$-\frac{dP}{dz} = \rho_m u_m \frac{du_m}{dz} + \rho_m g_z + \left(\frac{dP}{dz}\right)_{fr} + \left(\frac{dP}{dz}\right)_{fo} + \left(\frac{dP}{dz}\right)_{tp}$$
 (2)

$$\rho_m u_m A \frac{dh_m}{dz} = \left(\frac{d\dot{Q}}{dz}\right)_{in} \tag{3}$$

$$\left(\frac{dP}{dz}\right)_{fr} = \frac{f_v}{2D_h} \rho_m u_m^2 \tag{4}$$

$$f_a = C \operatorname{Re}_a^{-m} = C \left(\frac{\rho_a u_a D_h}{\mu_a} \right)^{-m} \tag{5}$$

$$x = \frac{h - h_f}{h_{fg}} = \frac{(h_{ini} + \Delta h) - h_f}{h_{fg}} = \frac{(h_{ini} - h_f) + \frac{1}{\dot{m}} \int q'' \xi dz}{h_{fg}}$$
(6)

$$\alpha = \left[1 + B_B \left(\frac{1 - x}{x} \right)^{n_1} \left(\frac{\rho_v}{\rho_I} \right)^{n_2} \left(\frac{\mu_I}{\mu_v} \right)^{n_3} \right]^{-1}$$
 (7)

$$\oint \frac{dP}{dz} = 0 \tag{8}$$

Table 1 Values of the constants used in equation (7)

Correlation or Model	$B_{\scriptscriptstyle B}$	n_1	n_2	n_3
Homogeneous model	1	1	1	0
Zivi model[4]	1	1	0.67	0
Wallis Separate Cylinder Model[5]	1	0.72	0.4	0.08
Lockhart and Martinelli[6]	0.28	0.64	0.36	0.07
Thom correlation[3]	1	1	0.89	0.18
Barocozy correlation[7]	1	0.74	0.65	0.13

2. Results and Discussion

2.1 Uniform channel gap

In many nuclear power plants, the reactor vessel is surrounded by a baffle structure (i.e., a thermal insulation structure) that forms a hemispherical annular flow channel with the vessel. Under the IVR-ERVC conditions during a severe accident, the channel acts as an engineered cooling system enhancing the natural circulation flow and increasing the corium cooling capacity of the system. Figure 1 shows an idealized channel with a uniform gap under consideration.

With the channel gap being uniform, the form loss by the geometric change of flow path in equation (2) is generated only at the inlet position. The loop integration of the form loss term can be expressed as follows:

$$\oint \left(\frac{dP}{dz}\right)_{fo} dz = \frac{K_{inlet}}{2} \rho_{inlet} u_{inlet}^2,$$
(9)

where the form factor K_{inlet} is taken to be 1.707 by considering the effects of sharp entrance [8]. Figure 2 shows the variation of void fraction with the mixture quality predicted by different correlations listed in Table 1. Figure 3 shows the induced mass flow rate using different void fraction models at the same inlet pressure of 2 bar, gap size of 0.1m, inlet diameter of 0.2m, uniform wall heat flux of 1MW/m², and saturated water condition. The Wallis Separate Cylinder model [5] estimates the lowest void fraction for a given mixture quality, so the induced mass flow rate is also the lowest as can be seen from Figure 3. For a conservative design, the Wallis Separate Cylinder model is used in later calculations.

Figures 4 and 5 show the variation of the mixture quality and void fraction along the channel height in the z-direction for different channel gap distances. It can be observed that for a fixed wall heat flux, the quality of two-phase flow is higher for a smaller value of channel gap size. This is expected as a reactor vessel with a smaller channel gap would accommodate a smaller induced mass of coolant fluid. For a given wall heat flux, a smaller mass would yield a higher quality. For the same channel gap, the quality increases rapidly in the hemispherical part of the channel as only the hemispherical channel, i.e., the lower head, is subjected to heating under severe accident conditions. The rate of increase is much slower in the vertical part as there is no heating. The magnitude and variation of void fraction along the channel are found to be quite similar for three different values of channel gap. Figure 5 shows that the void fraction is very sensitive to the change in the quality of the two-phase flow.

Figure 6 shows the effects of inlet diameter on the induced mass flow rate for heat flux values of 0.1 MW/m², 0.5 MW/m² and 1 MW/m², respectively. The inlet diameter strongly affects the induced mass flow since a smaller inlet diameter results in a larger pressure drop at the inlet. The inlet diameter is perhaps the most important limiting factor on the induced natural circulation, which in turn affects the coolability of the reactor vessel.

The effects of water subcooling at the inlet on the induced mass flow rate are shown in Figure 7. As the coolant temperature increases, the induced mass flow also increases. The water subcooling at the inlet is directly related to the coolant initial enthalpy. As the water subcooling decreases, the coolant initial enthalpy increases, which give rise to higher mixture quality and void fraction in the cooling channel subjected the same wall heat flux condition. A higher void fraction in the channel leads to a higher circulation mass flow.

Figure 8 depicts the effects of system pressure and water level (i.e., system height) on the induced mass flow rate at the heat flux level of 1MW/m^2 . A smaller value of induced mass flow rate is obtained for a higher system pressure. The effect of system pressure on the induced flow rate is brought about by its influence on the fluid properties; for instance the density of the liquid phase increases with the saturation pressure. A driving force for the natural circulation flow is the pressure difference between the liquid height H_o (see Figure 1) and an equivalent collapsed liquid height in the cooling channel. The pressure difference is larger for a larger value of H_o , so a considerably higher induced mass flow rate is obtained. The induced mass flow rate is sensitive to the total driving force available for the flow to be sustained which is directly proportional to the liquid height H_o . Hence the induced mass flow rate becomes higher for a larger value of H_o .

The effect of channel gap distance on the induced mass flow rate has been evaluated for different wall heat fluxes. Figure 9 shows the variation of the induced mass flow rate for heat flux levels of 0.1 MW/m², 0.5 MW/m², 1 MW/m², and 5 MW/m², respectively. It can be observed that the induced mass flow rate asymptotically approaches a constant value as the gap size increases. There is no further change in the induced mass flow rate for higher values of channel width since the internal flow now approaches the limiting case of an external flow. The mass flow rate is also dependent on the wall heat flux. For the limiting case of an external flow, a higher wall heat flux

is responsible in inducing a higher mass flow rate. If the induced natural circulation flow rate is small due to the small gap size, for example 0.025m, but the wall heat flux is extremely high, for example 5MW/m², then the induced liquid flow may be fully evaporated along the channel and the outlet flow would be superheated. Under superheated flow conditions, the induced mass flow rate can not be predicted since the superheated flow models have not been adapted to this paper.

It can also be observed from Figure 9 that for a given wall heat flux, the induced mass flow rate asymptotically increases with the gap size. So there exists a channel gap (i.e., an optimum gap size) for which the induced mass flow rate is largest. The induced mass flow rate can be fitted as an exponential function of the gap size as given below:

$$\dot{m} = \dot{m}_{\text{max}} - A \exp(-B/\delta) \tag{10}$$

An optimal gap size δ_{opt} is chosen as a gap which can generate 90% of the maximum induced mass flow rate, $0.9\,\dot{m}_{\rm max}$. The optimal gap sizes are calculated with the heat flux and inlet diameter as shown in Figure 10. As the wall heat flux and the inlet diameter increase, the optimal gap size tends to increase to accommodate a larger amount of vapour produced. Consequently the total induced mass flow rate for a higher heat flux and higher gap size is higher. Note that the optimal gap size is highly dependent on the inlet diameter since the pressure drop at the inlet is a dominant factor of the induced mass flow rate. The optimal gap size and the corresponding induced mass flow rate vary almost linearly with the wall heat flux as illustrated in Figure 10.

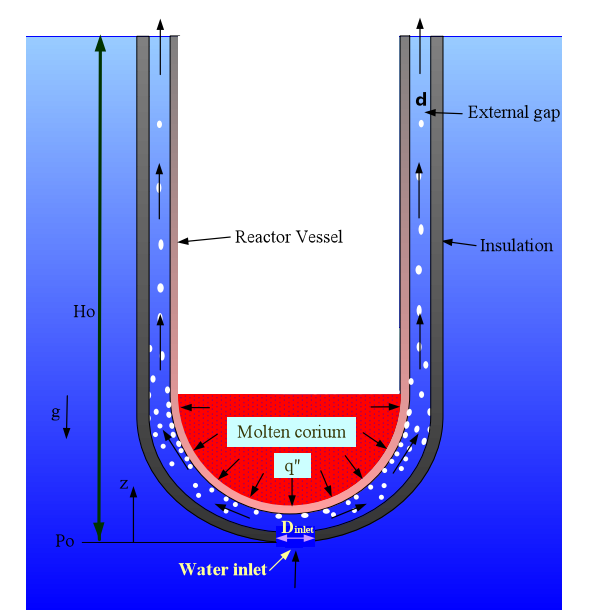


Figure 1. Schematic diagram of the reactor vessel with an idealized insulation structure

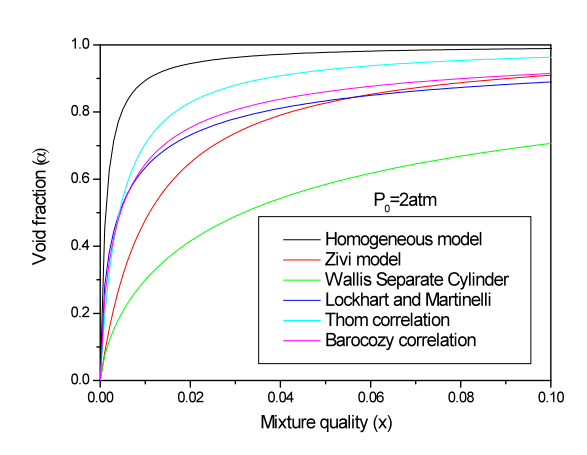


Figure 2. Variation of the void fraction predicted by different models

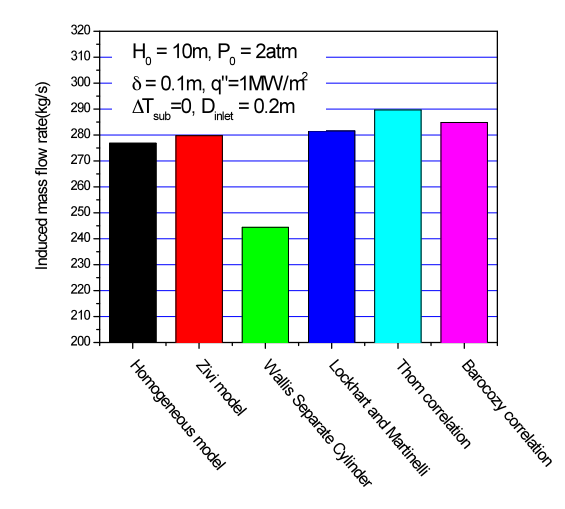
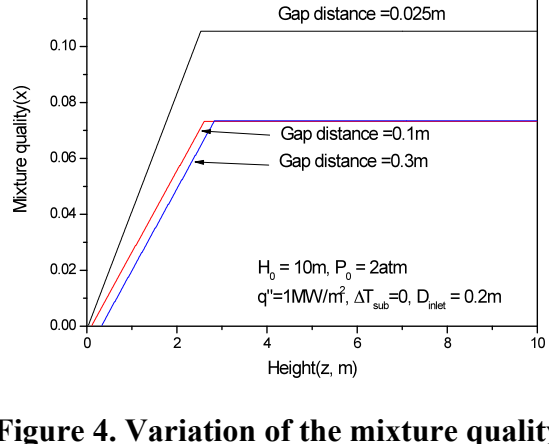


Figure 3. Variation of the induced mass flow rate using different void fraction models



0.12

Figure 4. Variation of the mixture quality along the channel height (z-direction)

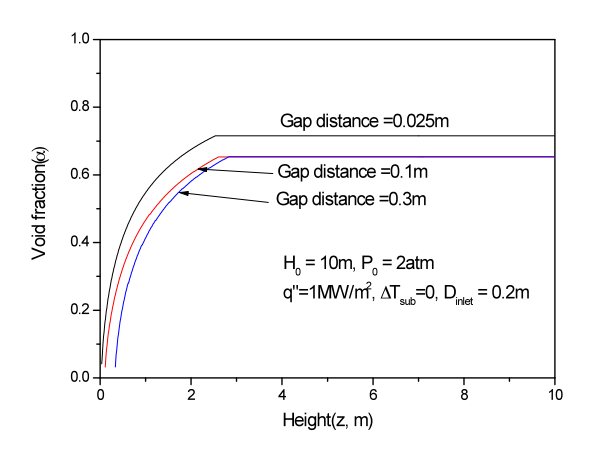


Figure 5. Variation of the void fraction along the channel height (z-direction)

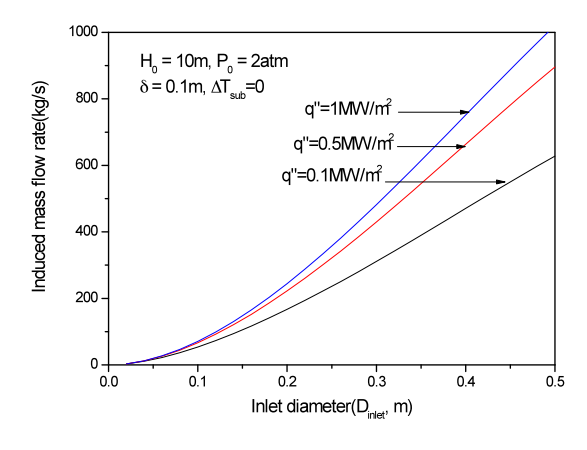


Figure 6. Variation of the induced mass flow rate with the inlet diameter

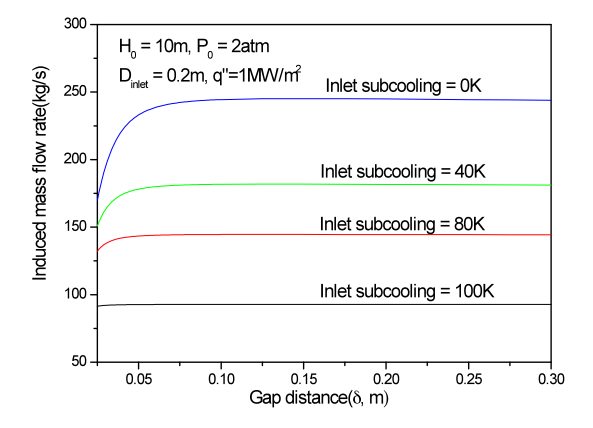


Figure 7. Effect of the inlet subcooling on the induced mass flow rate

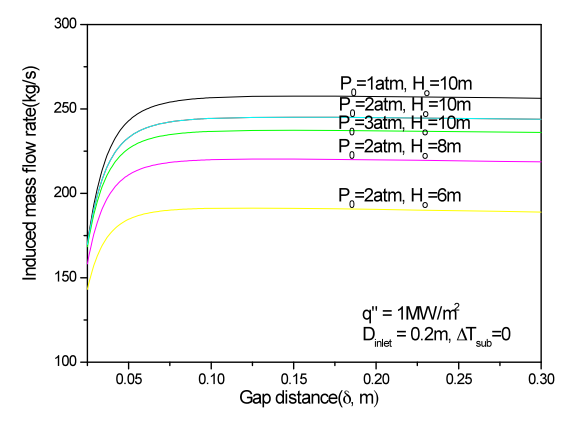
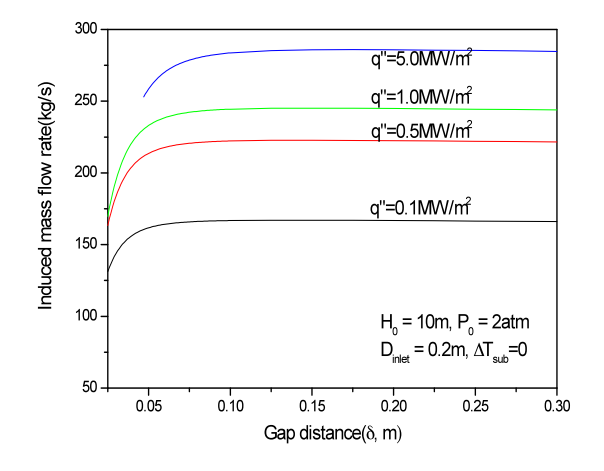


Figure 8. Effect of pressure on the induced mass flow rate



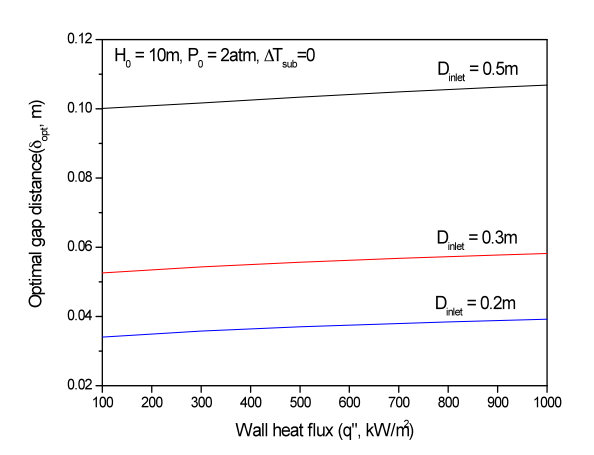


Figure 9. Effect of gap distance and heat flux on the induced mass flow rate

Figure 10. Optimal gap distance with heat flux and inlet diameter

2.2 Non-uniform channel gap

In an actual nuclear power plant such as APR1400, the channel gap size which plays an important role in the engineered cooling system should be varied along the height to enhance the natural circulation flow. Ha et al. [9] set up a one-dimensional facility to simulate a reactor vessel wall and its insulation, and performed experiments to observe the natural circulation mass flow by changing the ERVC design factors including the inlet/outlet area, the coolant outlet height, wall heating rate, water level, and water subcooling. The experimental model is shown in Figure 11. The main test section, which is a rectangular channel from a coolant inlet to a coolant outlet, simulates the natural circulation two-phase flow channel in the annular gap between the external reactor vessel and its insulation. One side of the rectangular channel is the reactor vessel wall and the opposite side is the insulation. The gap-size variation of the main test section along the height was determined by using Cheung's scaling analysis results [10] to scale down the reactor vessel height and the diameter of the APR1400. A channel width of 0.1m was employed for a one-dimensional flow channel. Consequently the main test section was scaled down to be a half height and 1/238 channel area of the APR1400 reactor. The coolant pool outside of the insulation device was maintained at a constant water level under the ERVC condition of the APR1400. There were two water tanks to supply a constant hydrostatic pressure head. One of the water tanks, the main tank, was connected to the coolant outlet port for a natural circulation of the coolant, and the other water tank was designed for a constant water level which could be controlled by changing the water level by using a float valve and a water drain hole.

In the work of Ha *et al.* [9], this experiment, the coolant inlet and outlet ports were installed in the insulation. A circular orifice was used for the coolant inlet port. The coolant inlet area was controlled by using various orifice diameters having the values of 16.0, 20.0, 28.3, 36.6, 49.1, and 67.4mm. The coolant outlet port was designed by boring a rectangular hole into the insulation wall. The experiments were carried out using a coolant outlet size of 43.6×81.8mm and an outlet height of 3.738m.

The primary form loss by the geometric change of flow path in the experimental facility is generated by the coolant inlet/outlet ports, the minimum gap, and the turbine flow meter position. Accordingly, the loop integration of the form loss term can be expressed as follows:

$$\oint \left(\frac{dP}{dz}\right)_{fo} dz = \frac{K_{inlet}}{2} \rho_{inlet} u_{inlet}^2 + \frac{K_{outlet}}{2} \rho_{outlet} u_{outlet}^2 + \frac{K_{\min}}{2} \rho_{\min} u_{\min}^2 + \frac{K_{tur}}{2} \rho_{tur} u_{tur}^2 \tag{11}$$

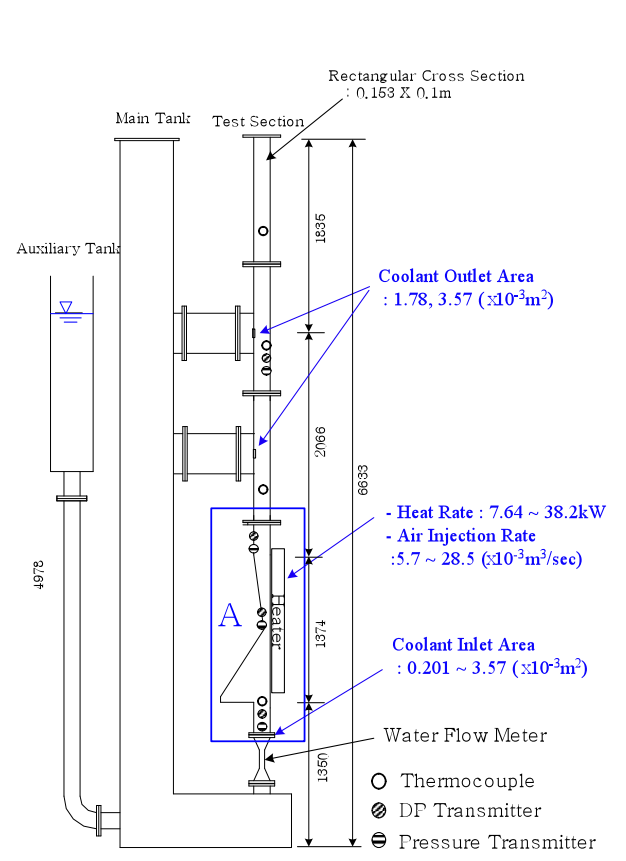


Figure 11. 1-D experimental facility with non-uniform gap [9]

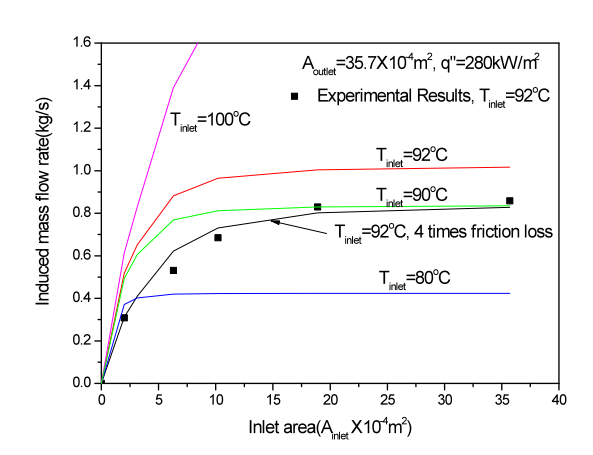


Figure 12. Comparison of 1-D experimental data with the calculated results

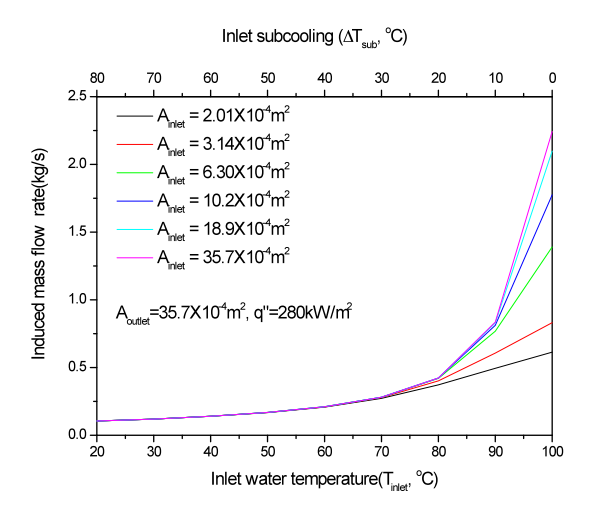


Figure 13. Effects of the inlet temperature on the induced mass flow rate

Considering the inlet/outlet port and the minimum gap as orifice and conversing-diverging transition pieces respectively, the shape factor correlations [8] of equations (12) to (14) are used. The calculated values of equation (15) result from applying the experimental system geometry. Through supplementary standard pressure drop tests, the experimental shape factor correlation for the turbine flow meter which has a representative diameter of 0.05m is used in equation (15) [1].

$$K_{inlet} \approx \left(1.707 - \frac{A_{inlet}}{A}\right)^2 \tag{12}$$

$$K_{outlet} \approx \left(1 + 0.707\sqrt{1 - \frac{A_{outlet}}{A}}\right)^2 \tag{13}$$

$$K_{\min} \approx 1.1(1 \times 0.66 \times 0.15 + 0)$$
 (14)

$$K_{tur} = 8.598 + 5.765 \exp\left(-\frac{\dot{m}}{2.084 [kg/sec]}\right)$$
 (15)

Figure 12 compares the induced mass flow rates measured by the experiment with the calculated results as a function of the inlet area for an average heat flux of 280kW/m² and inlet coolant temperature of 92 °C. Figure 13 shows the effects of the inlet water temperature on the induced mass flow rate. In the experiment, it was observed that the induced mass flow rate and the inlet and wall temperatures had fluctuated periodically. This was due to the variations of the water boiling rate and the wall heat transfer rate. As the wall temperature increased, the water boiling rate on the heated wall also increased. The experimental flow rates shown in Figure 12 are time-averaged ones. Even though the predicted circulation mass flow rate is obtained by assuming steady state flow condition, the predicted flow rate is similar to the experimental one. Figure 12 also shows the predicted flow rates by assuming four-time larger friction loss term, and the flow rates with larger friction losses predict the experimentally measured values accurately. Evidently, the friction loss modelling is very important in predicting the induced mass flow rate in a channel having non-uniform gap size.

2.3 Inclined channel

Song et al. [11] proposed an ex-vessel core catcher concept which can be adapted for both existing reactors and advanced light water reactors. It is a passively actuating device which can arrest and stabilize the molten core material inside the reactor cavity. The primary goal of the proposed ex-vessel core catcher is to reliably accommodate and rapidly stabilize the corium, including the entire core inventory and reactor internals that is injected into the cavity following a postulated severe accident. To achieve this important goal, the proposed core catcher design employs the combined effects of several key design components to: (i) direct the paths of relocation of the corium once the accident proceeds to the ex-vessel stage, (ii) retain the corium within the ex-vessel core catcher, (iii) promote spreading of the corium over the entire floor area of the core catcher, and (iv) provide effective long-term cooling of the corium so as to quickly achieve and maintain a stabilized corium configuration. These key design components include: (1) a composite layer of sacrificial material and protective material, (2) a corium spreading compartment, and (3) an engineered corium cooling system with passive natural circulation.

As shown in Figure 14, the core catcher body made of carbon steel is to be placed inside the reactor cavity below the reactor vessel. Molten corium discharged from the reactor vessel is to be collected and spread inside the core catcher body having a composite layer of sacrificial materials located on top. The core catcher provides a feature for a natural circulation driven cooling, which is schematically shown in the figure. The cooling channel is made of a single

channel between the core catcher body and the inside wall of the reactor cavity. A large number of short columnar structures, i.e. studs, are placed between the core catcher body and the reactor cavity wall, which are used to withstand the static and dynamic loading on the core catcher body. The design parameters including the size of the gap, spacing between the studs, thickness of the sacrificial material, thickness of the protection material will be determined during the design process. The cooling channel has an inclination angle of ~10 degree to facilitate the steam venting. The gap size towards the exit of the cooing channel can be increased to further promote steam venting. The arrangement of studs in a square pattern, with the possibility of optimization on the shape and geometric arrangement, is to be left open. A down-comer is provided to result in a two-phase natural circulation. In the conceptual design, a rectangular dividing wall provides a separation between the down-comer channel and the cooling channel. Detailed design and arrangement of down comers are left open.

The cooling channel in the core catcher is treated as two-dimensional with a gap size of 0.1m, a width of 6m, a depth of 16m, and an angle of inclination of 10 degrees. The inlet water box having a width of 0.6m is located at the bottom of the core catcher for the coolant flowing from the IRWST and the downcomer. The induced mass flow rates are estimated from which the design criteria are set up for the inlet box and the studs in the cooling channel. The form loss by the inlet water box and the studs can be described by equation (15). It is assumed that there are several inlet holes in the water box. The quantity N_{inlet} represents the number of inlet holes in equation (16). The form factor K_{inlet} at unit hole is selected as 1.707 by considering the effects of sharp entrance [8]. The form loss by the studs is defined at the entrance of the inclined channel.

$$\oint \left(\frac{dP}{dz}\right)_{fo} dz = N_{inlet} \frac{K_{inlet}}{2} \rho_{inlet} u_{inlet}^2 + \frac{K_{stud}}{2} \rho_{stud} u_{stud}^2 \tag{16}$$

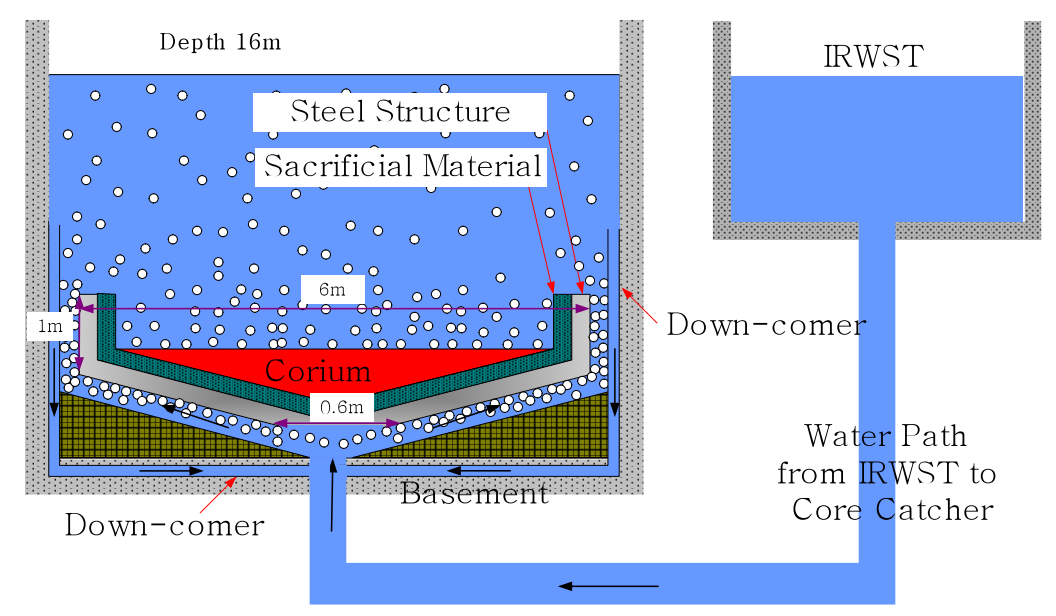
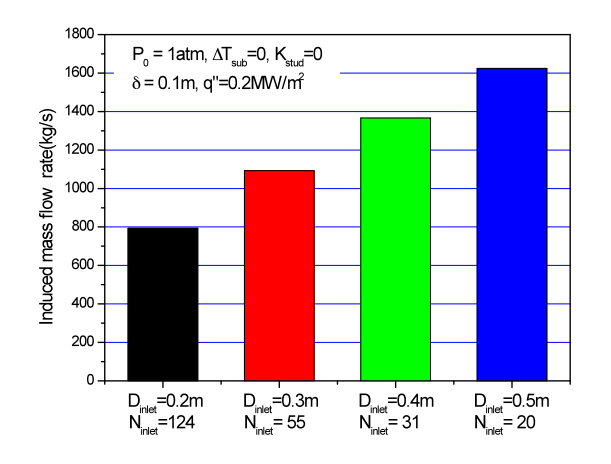


Figure 14. Core catcher concept with natural circulation

Figure 15 shows the effect of the inlet configurations on the induced mass flow rates for the same total inlet area of 3.9m². Because the total inlet area is the same, there are a large number of

holes in the water box if the hole diameter is smaller. The induced mass flow rate increases as the hole diameter increases since the form factor and flow velocity at unit hole decrease.

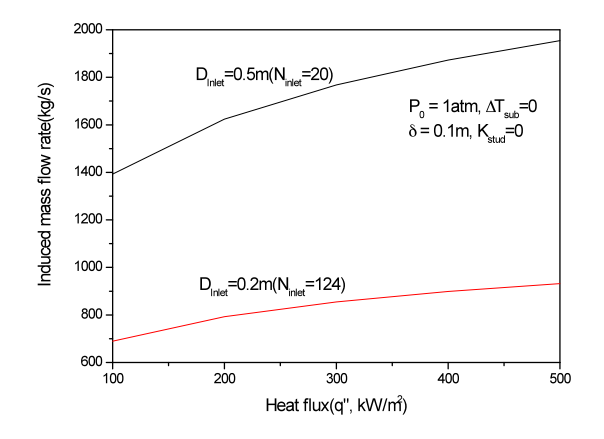
Figures 16 and 17 depict the effects of the inlet subcooling and wall heat flux, respectively. If the inlet subcooling is smaller than about 20°C, the induced mass flow rate increases abruptly. As shown in Figure 16, the inlet configuration has no effects on the induced mass flow rate when the inlet subcooling is larger than 15°C. This is because the induced mass flow rate is limited by the subcooling. A larger subcooling leads to a smaller void fraction and a smaller driving force. As shown in Figure 17, the induced mass flow rate increases as the wall heat flux increases. However the inlet configuration has a stronger effect on the induced mass flow rate.

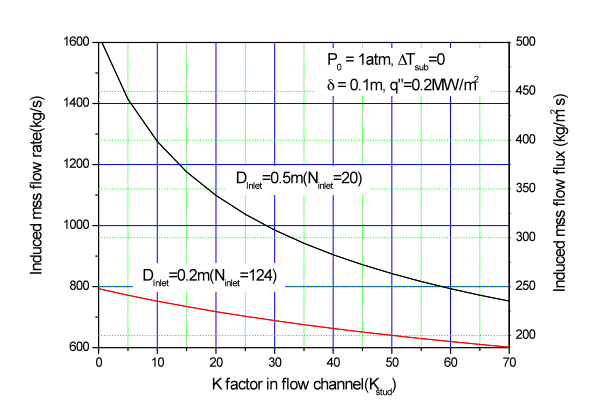


1800 $P_0 = 1atm, K_{stud} = 0$ 1600 $\delta = 0.1 \text{m}, \text{ q}'' = 0.2 \text{MW/m}^2$ Induced mass flow rate(kg/s) 1400 1200 1000 D_{Inlet}=0.5m(N_{inlet}=20) 800 $D_{inlet} = 0.2 \text{m} (N_{inlet} = 124)$ 600 400 200 O 30 Inlet subcooling($\Delta T_{_{\text{sub}}}$

Figure 15. Effect of the inlet configuration on the induced mass flow rate

Figure 16. Effect of the inlet subcooling on the induced mass flow rate





induced mass flux

Figure 17. Effect of the wall heat flux on the Figure 18. Effect of the form factor by studs on the induced mass flux

Figures 15 to 17 are obtained by assuming no flow resistance by the studs. Figure 18 shows the effect of the form factor on the induced mass flow rate. The design of the studs including the spacing between the studs, the shape of the stud, and the number of the studs is an important and crucial factor in determining the induced mass flow rate, and finally cooling capacity of the core catcher. According to Figure 18, the water box should be designed to have 20-unit hole with a diameter of 0.5m whereas the studs be designed to have less than form factor of 50 if the induced mass flow rate per unit channel area (i.e., the induced mass flux) is expected to generate up to $200 \text{kg/m}^2 \text{ s}$.

3. Summary and Conclusions

The boiling-induced natural circulation flow in the engineered cooling channel has been modelled by considering the conservation of mass, momentum and energy in the two-phase mixture, along with the two-phase friction drop and void fraction. The resulting governing system has been solved numerically to predict the natural circulation flow rate that would be induced in the channel by the downward-facing boiling process with the flow area and the inclination of the channel relative to the gravitational field as the key parameters.

The model has been applied to estimate the induced mass flow rates through a uniform annular gap between the reactor vessel and insulation under the IVR-ERVC conditions during a severe accident for various values of the channel gap size, inlet diameter, inlet subcooling, and wall heat flux. A higher induced mass flow rate is obtained for a higher wall heat flux, a larger gap size, a larger inlet diameter, and a smaller subcooling. In particular, the optimal gap size is found to be highly dependent on the inlet diameter since the pressure drop at the inlet is a dominant factor for the induced mass flow rate. The optimal gap size and the corresponding induced mass flow rate vary almost linearly with the wall heat flux.

For more realistic IVR-ERVC conditions with non-uniform gap sizes, the induced mass flow rate has been calculated and compared with experimental data. The induced mass flow rate is found to be strongly affected by the inlet subcooling. In addition, the friction loss modelling is found to be very important in predicting the induced mass flow rate in a channel having non-uniform gap sizes.

The model has also been applied to predict the performance of the engineered corium cooling system of an ex-vessel core catcher. Specifically, the induced mass flow rates have been estimated for given inlet configuration, inlet subcooling, wall heat flux, and form factor by the studs in the cooling channel. Appropriate design criteria for the water inlet box and the studs have been determined in order to achieve the required induced mass flow rates.

4. References

- [1] J. C. Kim, K. S. Ha, R. J. Park, S. B. Kim, and S. W. Hong, "Loop analysis of a natural circulation two-phase flow under an external reactor vessel cooling", International Communications in Heat and Mass Transfer, Vol.35, 2008, pp.1001-1006.
- [2] D. Butterworth, "A Comparison of Some Void-Fraction Relationships for Co-Current Gas-Liquid Flow", International Journal of Multiphase Flow. Vol.1, Issue 6, 1975, pp.845-850.

- [3] J. R. S. Thom, "Prediction of Pressure Drop During Forced Circulation Boiling of Water", Int. J. Heat and Mass Transfer. Vol. 7, Issue7, 1969, pp.709-724.
- [4] S. M. Zivi, "Estimation of Steady-State Steam Void-Fraction by Means of the Principle of Minimum Entropy Production", Journal of Heat Transfer. Vol.86, pp.247-252, 1964.
- [5] G. B. Wallis, One-Dimensional Two-Phase Flow, McGraw-Hill New York, 1969.
- [6] R. W. Lockhart, and R. C. Martinelli, "Proposed Correlation of Data for Isothermal Two-Phase, Two-Component Flow in Pipes", Chemical Engineering Progress. Vol.45, No.1, 1949, pp.39-48.
- [7] C. J. Baroczy, "Correlation of Liquid Fraction in Two-Phase Flow with Application to Liquid Metals", Chemical Engineering Progress Symposium Series. Vol.61, No.57, 1965, pp.179-191.
- [8] I.E. Idelchik, Handbook of Hydraulic Resistance, 3rd Ed., Begell House, New York, 1994, pp.171, pp.319, pp.688.
- [9] K. S. Ha, J. C. Kim, R. J. Park, S. B. Kim, and S. W. Hong, "One-dimensional Study on the Two-Phase Natural Circulation Flow on an External Reactor Vessel Wall", <u>Proceedings of the 7th International Topical Meeting on Nuclear Reactor Thermal Hydraulics, Operation and Safety</u>, Seoul, Korea, 2008, Oct. 5-9.
- [10] F. B. Cheung and L. C. Liu, "CHF Experiments to Support In-Vessel Retention Feasibility Study for an Evolutionary ALWR Design", EPRI WO# 5491-01, PSU/MNE-99-263J, 1999.
- [11] J. H. Song, H. Y. Kim, K. S. Ha, R. J. Park, J. T. Kim, and F. B. Cheung, "A Core Catcher Design for the Advanced Light Water Reactor", <u>Proceedings of ICAPP</u>, Nice, France, May 2-5, 2011.

Nomenclature

A: cross-section area(m²) D_h : hydraulic diameter(m) g: gravitational acceleration(m/s²) f: wall friction factor f: wall friction factor f: induced mass flow rate(kg/s) f: pressure(N/m²) f: wall heat flux (w/m²) f: wall heat flux (w/m²) f: vertical coordinate(m)

Greek symbols

 α : void fraction δ : gap distance(size) (m) ρ : density(kg/m³) $\Delta \rho$: density difference between phases(kg/m³) μ : viscosity(kg/m·s) ξ : perimeter(m)

Subscripts

f: liquid phasefr: friction lossfo: form lossg: gas phase

The 14th International Topical Meeting on Nuclear Reactor Thermal Hydraulics, NURETH-14 Toronto, Ontario, Canada, September 25-30, 2011

m : mean mixture property min : value at minimum gap *inlet*: value at inlet *max* : maximum value opt: optimal value outlet: value at outlet

tp : two-phase loss *tur*: value at the turbine flow meter